FEDERAL UNIVERSITY OF AMAZONAS - UFAM

INSTITUTE OF COMPUTING - ICOMP

POST-GRADUATE PROGRAM IN INFORMATICS - PPGI

Indoor Positioning System Using Dynamic Model Estimation

Yuri Freitas Assayag

Manaus - AM

March 2021

Yuri Freitas Assayag

Indoor Positioning System Using Dynamic Model Estimation

A master thesis submitted to the Post-graduate Program in Informatics of the Institute of Computing of the Federal University of Amazonas in partial fulfillment of requirements for the degree of Master of Science. Concentration area: Informatics.

Advisor

Horácio A. B. Fernandes de Oliveira, D.S.c

FEDERAL UNIVERSITY OF AMAZONAS - UFAM

INSTITUTE OF COMPUTING - ICOMP

Manaus - AM

March 2021

Ficha Catalográfica

Ficha catalográfica elaborada automaticamente de acordo com os dados fornecidos pelo(a) autor(a).

Assayag, Yuri Freitas
A844i Indoor Positioning System Using Dynamic Model Estimation : system using dynamic model estimation / Yuri Freitas Assayag . 2021
52 f.: 31 cm.

Orientador: Horácio Antonio Braga Fernandes de Oliveira
Dissertação (Mestrado em Informática) - Universidade Federal do Amazonas.

1. Indoor Positioning System. 2. Path-loss Model. 3. Bluetooth Low Energy. 4. Trilateration. I. Oliveira, Horácio Antonio Braga Fernandes de. II. Universidade Federal do Amazonas III. Título

FOLHA DE APROVAÇÃO

"Indoor Positioning System Using Dynamic Model Estimation"

YURI FREITAS ASSAYAG

Dissertação de Mestrado defendida e aprovada pela banca examinadora constituída pelos Professores:

Prof. Horácio Antônio Braga Fernandes de Oliveira - PRESIDENTE

Prof. Richard Werner Pazzi - MEMBRO EXTERNO

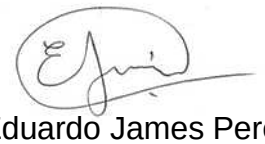

Prof. Eduardo James Pereira Souto - MEMBRO INTERNO

Manaus, 31 de Março de 2021

Acknowledgements

First of all, I would like to thank God for the strength to overcome difficulties, for health, and for all your grace in my life.

I would like to thank my family, especially my parents Rosalvo and Karla for all the support during my academic life and for the sacrifices they made so that I could reach this stage of my life. I thank my grandmother Cleide, my uncles Virle, Jocicleide and Claudia, my brothers Matheus and Maria Eduarda, because they make me a better person every day, and also thanks to my sister-in-law Beatriz Bruna that helped me to revise my articles in English.

I want to thank the Federal University of Amazonas, in particular, the Institute of Computing for all the teaching I have been given and its excellent faculty. A special thanks to my advisor professor Horácio Fernandes for all the guidance, availability, and opportunities.

I am grateful for the support given by the Coordination for the Improvement of Higher Education Personnel (CAPES), by the Institute of Innovation, Research and Scientific and Technological Development of Amazonas (IPDEC), by Positivo Technologies and by Samsung Electronics da Amazônia Ltda, through the agreement no 003, signed with ICOMP / UFAM that allowed this work to be carried out.

And last but not least, I want to thank all my laboratory friends for their tips during this researcher process, for helping with experiments and exchanging experiences, and to all my colleagues and friends who were part of this stage of my life.

Indoor Positioning System Using Dynamic Model Estimation

Autor: Yuri Freitas Assayag

Orientador: Horácio A. B. Fernandes de Oliveira, D.S.c

Abstract

Indoor Positioning Systems (IPSs) are used to locate mobile devices in indoor environments. Model-based IPSs have the advantage of not having an exhausting training and signal characterization of the environment, as required by the fingerprint technique. However, most model-based IPSs are done using static model parameters, treating the whole scenario as having a uniform signal propagation. This might work for most small scale experiments, but not for larger scenarios. In this work, we propose PoDME (Positioning using Dynamic Model Estimation), a model-based IPS that uses dynamic parameters that are estimated based on the location the signal was sent. More specifically, we use the set of anchor nodes that received the signal sent by the mobile node and their signal strengths, to estimate the best local values for the propagation model parameters. Also, since our solution depends highly on the selected anchor nodes to use on the position computation, we propose a novel method for choosing the three best anchor nodes. Our method is based on several data analyses executed on a large-scale, Bluetooth-based, real-world experiment and it chooses not only the nearest anchor but also the ones that benefit our least-square-based position computation. Our solution achieves a position estimation error of 3 m, which is 17% lower than the position estimates obtained by positioning models based on static parameters.

Keywords: Indoor Positioning Systems; Bluetooth Low Energy; Path-loss Model; Localization Systems, Trilateration.

List of Figures

List of Tables

List of abbreviations and acronymns

AoA Angle of Arrival

BLE Bluetooth Low Energy

BPNN Back Propagation Neural Network

GNSS Global Navigation Satellite Systems

GPS Global Positioning System

IoT Internet of Things

IPS Indoor Positioning Systems

ITU International Telecommunication Union

PoDME Positioning using Dynamic Model Estimation

RFID Radio Frequency Identification

RMSE Root Mean Square Error

RSSI Received Signal Strength Indicator

TDoA Time Difference of Arrival

ToA Time of Arrival

UWB Ultra-Wide Ban

WLS Weighted Least Squares

List of symbols

α triangle alpha angle

β triangle beta angle

Δ threshold proximity to equilateral triangle

η path-loss exponent

γ triangle gamma angle

$R0$ RSSI value in 1 meter

X_σ zero-mean Gaussian random variable

Contents

1 Introduction

Today's most commonly used positioning system is the Global Navigation Satellite Systems (GNSS), which includes the Global Positioning System (GPS). They allow people to navigate from place to place through applications such as Google Maps, Waze, and Apple Maps. However, the satellite signals are easily blocked by buildings, decreasing its accuracy, and making its usage limited to outdoor environments (Ni et al., 2006). For this reason, Indoor Positioning Systems (IPSs) have been proposed to allow the location of mobile devices indoors, using the local infrastructure.

IPSs have been drawing the attention of many companies since it allows the development of several interesting applications, such as monitoring the position of the elderly in retirement homes, monitoring children in schools, assisting customers in supermarkets, and tracking patients and equipment in hospitals (Brena et al., 2017).

Many IPSs have been proposed in the literature, but to date, no system has been established as standard since each one has its pros and cons. Positions can be estimated using several data sources, such as the Angle of Arrival (AoA), Time of Arrival (ToA), Time Difference of Arrival (TDoA), and the Received Signal Strength Indicator (RSSI). However, most IPS solutions are based on the RSSI due to its low cost and high availability since they can use signals from WiFi and Bluetooth, both of which are available in most mobile devices (Sadowski and Spachos, 2018).

The RSSI can be used to estimate the distance between two devices since there is a decrease in the signal strength as the distance increases (Li et al., 2018). However, the RSSI is sensitive to environmental noises, such as obstacles from furniture and walls, people's movements, and opening or closing doors, all of which can cause a high signal variation making it difficult to convert the signal strength to distance accurately (Sadowski and Spachos, 2018). Consequently, the position estimation of the

mobile device is affected.

Many wireless communication technologies can be used in IPS, such as WiFi and Bluetooth, as mentioned, but also Radio Frequency Identification (RFID), Ultra-Wide Ban (UWB), ZigBee, and others. WiFi has greater prominence since it is the most used technology and, therefore, more easily found indoors, which results in no need for extra hardware (Torteeka and Chundi, 2014). However, WiFi consumes more energy, making it unfeasible for small, low-power devices (Zuo et al., 2018). Thus, with the development of BLE, it has become increasingly common to employ this technology due to its low energy consumption, ease of deployment, and low cost (Faragher and Harle, 2015).

IPSs can be classified into two categories: fingerprint-based and model-based. Fingerprint-based IPSs use an extensive and exhaustive training of reference points in the scenario to feed a machine learning algorithm that will later be used to localize the mobile devices. The created signal map is susceptible to changes in the environment (He and Chan, 2016) and is unfeasible to be generated and maintained for larger scenarios. On the other hand, model-based IPSs require only some information from the scenario, such as the coordinates of the anchors (reference nodes) and, in some cases, a simple collection of signal data, to create a better signal propagation model for the scenario.

The model-based IPSs have two main phases: model data gathering and position computation (Wu et al., 2019). In the first phase, RSSI samples are taken to obtain the signal propagation model (also known as path-loss model) that characterizes the signal strength in the scenario as the distance increases. This is the most sensitive step since it depends directly on the measured RSSI values in the real environment, which are known to have a high variance, and they will also affect the estimated distances (Li et al., 2018). In the position computation phase, the positions of the mobile devices are computed using the distances estimations and the known position of the anchors. This computation is usually done by some optimization algorithms, such as the least-squares (Teoman and Ovatman, 2019).

Most model-based IPSs proposed in the literature use the same static model parameters for the whole scenario (Fang and Chen, 2020; Shi et al., 2017; Teoman and Ovatman, 2019; Yong et al., 2020). This static model considers that the signals

behave uniformly over the whole scenario. However, this is not the case, especially for medium to large-scale scenarios in which the signal behavior changes from place to place depending on the obstacles and other environment variables. In this work, we propose PoDME (Positioning using Dynamic Model Estimation), an IPS that uses a signal propagation model with dynamically estimated parameters to improve the distance computation between the mobile device and the anchor nodes. Our main idea is that these dynamically estimated path-loss parameters correspond more closely to the signal's characteristics of the region where the packet we want to localize was sent from, improving the accuracy of the estimated distances. Also, since our solution depends highly on the selected anchors used on the position computation, we propose a novel method for choosing the three best anchors that focus not only on the nearest anchors but also the ones that benefit the least-squares-based position computation.

In our experiments, we decided to use the BLE technology. We implemented our solution in a real-world, large-scale testbed and compared its performance to different variations of a static model-based IPS, as used by most model-based solutions in the literature. Our results show an average error of 3 m, a 17% improvement compared to the best experimented parameter of a static model-based IPS, which had an error of 3.6 m.

1.1 Objectives

The main goal of this work is to develop and evaluate a IPS to be implemented in medium to large-scale scenarios that uses a signal propagation dynamic model to provide location information for small battery-powered devices to be worn by people inside buildings, such as the elderly in retirement homes or students in schools.

As specific objectives, it is intended:

- Establish the signal collecting method from the environment to obtain consolidated data that support the proposed approach;
- Evaluate and improve the smoothing filter for reducing noise from RSSI;

- Implement a propagation model with a dynamic choice of the parameters using information from different regions of the environment;
- Propose a novel method for choosing the best anchor nodes that benefit the least-squares-based position computation;

1.2 Structure of the Master Thesis

The rest of this master thesis is organized as follows: Chapter 2 gives a theoretical background for this IPS proposed, shows the different technologies, localization techniques, and works that are directly related to the development of this work. In Chapter 3, we present our proposed PoDME solution, show the components of our system and explain the offline and online phases. Chapter 4, presents the performance evaluation of our solution in a real-world testbed, and shows the comparison of different methods. Finally, in Chapter 5, summarises the results and suggestions for future work.

2 Frame of Reference

This chapter presents the theoretical background for this IPS proposed. We show different technologies, localization techniques, and works that are directly related to the development of this work.

2.1 Bluetooth Low Energy

The BLE is currently available on most electronic devices, such as smartphones, notebooks, and Internet of Things (IoT) devices. Due to this availability and the focus on low energy consumption, this technology has become attractive for use in indoor location systems and has become increasingly common in several works (Dickinson et al., 2016; Onofre et al., 2016; Paterna et al., 2017; Zhuang et al., 2016). With the advances in BLE, an improved Bluetooth version, it has been possible to obtain a more significant reduction in cost while also reducing the power consumption, ensuring an increased lifespan for the devices (Zhuang et al., 2016). Also, BLE introduced the advertisement packets, which are data packets used mainly for positioning, in which the receiving devices are required to report the RSSI.

BLE devices can communicate with each other and, in this way, it is possible to establish an ad-hoc network composed of several nodes. As the number of network nodes increases, the interference among devices increases. To reduce this interference, BLE performs a channel division and makes a random jump among them, changing frequency between 2.402 GHz and 2.480 GHz (Al Kalaa and Refai, 2015).

2.2 Multipath

Wireless communication takes place through signal emitting and receiving devices. When a transmitter sends a signal through a wireless channel, waves propagate in different ways due to reflections caused by room layout. Several devices adopt omnidirectional antennas, which propagate signals in all directions. Thus, the same signal will arrive in different ways at the receivers depending on the objects and the line-of-sight between them.

The reflected signal will always have a phase change compared to the signal emitted in a direct line between two devices. Such a phase change causes attenuation in the signal, and this effect is called multipath. All wireless communication is affected by this effect, however, communication in indoor environments is more affected due to the greater number of obstacles present in the environment, being therefore responsible for the high variation in signal strength (Sadowski and Spachos, 2018).

The signal variation can be increased by devices motions, called the doppler effect. To decrease the signal variation, some authors suggest the filters use such as the mean filter (Luo and Zhan, 2014), particle filter (Liu et al., 2019), and Kalman filter (Sung, 2016). The sliding window filter also proved to be a simple solution with some of the best results.

2.3 Log-Distance Path Loss Model

In IPSs, the RSSI can be used to estimate the distance between mobile devices to anchor nodes. The RSSI is highly dependent on the environment in which the electromagnetic wave will propagate and gradually decreases when the devices are moved away.

The IPS uses the RSSI as information for positioning mainly due to the simplicity and low cost for the system's implementation, as this is information available in all wireless communication devices. In free space, the signal loss is low, however, according to the obstacles in the environment and the multipath effects that wave suffers, the signal variation becomes high, decreasing the IPS accuracy that uses RSSI values (Glitza et al., 2017).

The relationship between signal and distance can be represented using a signal propagation model. Thus, because the RSSI value decreases with increasing distance and it is affected by the multipath, the most used propagation model to model the relationship between signal and distance is the log-distance path loss model. This model is given by the following equation:

$$R(d) = R_0 - 10\eta \log_{10} \frac{d}{d_0} + X_\sigma \tag{2.1}$$

where d is the distance between the transmitter and the receiver, $R(d)$ is the RSSI value measured at distance d, $R0$ is the RSSI value measured at distance d_0, η is the path-loss exponent, i.e., a signal loss rate related to the environment and, finally, X_σ is a zero-mean Gaussian random variable (Huang et al., 2019) that models the RSSI variation. For the d_0 model parameter, a distance of 1 m is commonly used in the literature (Chan and Sohn, 2012; Yong et al., 2020). Thus, R_0 is the RSSI at 1 m.

As each scenario of using an IPS contains layouts with different obstacles, the parameters' values $R0$ and η tend to vary, requiring minimal training to be obtained correctly.

2.4 Positioning Techniques

2.4.1 Angle of Arrival (AoA)

Angle of Arrival is a location technique that uses information from the angles that the signals arrive at a set of antennas on the anchor nodes. Through the arrival angle information, the positioning calculation can be done through algorithms that cross this information and compare the line's intersections to find the device coordinates (Tariq et al., 2017). In this technique, the anchor nodes must know in advance their orientation to make the positioning calculation.

This technique is affected by multipath and depends on the layout and materials of the environment. To reduce the multipath effect on the signal behavior, a large number of antennas more sensitive to signal orientation are used, which adds greater positioning accuracy but also increases the hardware complexity (Brena et al., 2017).

2.4.2 Time of Arrival (ToA)

Time of Arrival is a location technique that estimated the distance between two devices using the RTT, measurement the signal propagation time in the transmitter-receiver direction, and multiplies this value by the propagation speed that the electromagnetic wave travels, i.e., the light speed. This technique requires devices with a synchronized clocks, as any synchronization failure can result in greater positioning errors (Lim et al., 2007).

This is one of the techniques that achieve the smallest positioning errors, making it one of the most accurate techniques, although the multipath that the wave travels can interfere with the distance accuracy. However, due to the need and the cost of hardware with high time synchronization, this technique becomes a challenge to be used in IPSs (Tariq et al., 2017).

2.4.3 Proximity

This technique can also be referred to as the source cell, as a reference anchor is needed to estimate the location of the target to be tracked through the proximity between them (Liu et al., 2007). For this, it is necessary to spread several reference anchors around the environment, with their location duly known by the system.

The basic case of tracking with this technique is when the device location is requested, and it is detected by only one anchor. In this case, it can be said that the device is close to the anchor. When more anchors detect the device, then the anchor that had the strongest RSSI is chosen as the closest (Dickinson et al., 2016).

This technique is generally used when it is necessary to obtain precision by room and a simple implementation is required. For cases in which it is necessary to obtain precision by point inside the room, this technique becomes a bad choice.

2.4.4 Fingerprint

The fingerprint is a technique that consists of obtaining the scenario characteristics through signals fingerprints, thus forming a signal map. The fingerprint is done through the RSSI and this technique implementation has two phases: offline and online.

During the offline phase, an analysis of the scenario is made, separating the environment into several reference points and for each point are collected some RSSI values by the anchors nodes (He and Chan, 2016). The values obtained at each point are stored in an offline database that will be used to obtain the location later.

During the online phase, the system obtains signals values emitted by the tracking device and compares these values with those collected in the offline phase, verifying which reference point is more similar to the newly received signal, and thus the positioning is estimated (Faragher and Harle, 2015).

The fingerprint method is more accurate than model-based solutions, but it is time-consuming since it requires the characterizations of the environment through the signal map. Also, this method is susceptible to changes in the environment, such as the number of people, new walls, and furniture, that require a new characterization of the signals.

2.4.5 Trilateration

Trilateration (also called a model-based technique), is a traditional technique to estimating the device position through the distances to three reference anchors with previously known positions. As with the fingerprint-based IPSs, the main information used in model-based IPSs is the RSSI. However, it is well-known that the signal strength value varies widely, either due to the nature of the wireless channel or some obstacles in the environment (Ji et al., 2006; Yong et al., 2020). This problem is worse in the packet losses presences, especially when using BLE advertising packets, in which only half of the packets are usually received.

The distances used are obtained through the RSSI transformation to distance made by propagation models such log-distance path-loss model. Thus, each reference

anchor will have a circle of radius equal to the estimated distance and the device position can be estimated through the circumferences intersection.

The circumferences intersection will only be formed in an ideal scenario, in which the distance is perfectly estimated by the RSSI. However, this does not occur in a real scenario due to the variations in signal strength caused by multipath. To solve this problem, optimization algorithms are used that find a point that minimizes the distance to all reference anchors, such as the least-squares method (Ni et al., 2006; Shi et al., 2017; Zhou et al., 2017). When more than three reference anchor are used in the positioning calculation, we call it multilateration.

2.5 Related Work

Among the RSSI-based methods, the nearest-anchor method is possibly the most simple solution. The works of Wu et al. (2019), and Dickinson et al. (2016), compare the nearest-anchor with other model-based techniques.

In the fingerprint technique, training of the whole scenario is required to generate an RSSI database that will be used by machine learning algorithms to estimate positions in the online phase. The positioning system developed by Bahl and Padmanabhan (2000), called RADAR, is a classic work in the area because it was one of the first to create a signal map using RSSI. The solution proposed by the authors resulted in an accuracy of 2 m to 3 m.

Model-based IPSs use propagation models to transform the RSSI value in the distance between the sender and receiver. Such propagation models try to model the behavior of the signal in relation to the variation of distance. In Onofre et al. (2016), the authors developed an empirical propagation model using the RSSIs collected from a real-world experiment to estimate the distance based on the signal strength. However, the proposed propagation model is valid only for the experimented site.

In Li et al. (2018), it was proposed an IPS that uses a distance-based RSSI adjustment model to correct signal losses in the environment. The work compares three main propagation models: Log-Distance, Back Propagation Neural Network (BPNN), and

Back Propagation Neural Network with a Particle Swarm Optimization (PSO-BPNN). Their experiment is performed in a small-scale scenario with an area of 9×6 m^2, consisting of four anchor nodes, an Android-based mobile device, and a gateway. The proposed solution resulted in a Root Mean Square Error (RMSE) of 2 m when using PSO-BPNN. However, these results were obtained by evaluating only 8 reference points and without considering the corners of the scenario as well as other regions with more complex signal behaviors, with more obstacles, and low anchors nodes coverage.

The system proposed by Wu et al. (2018), called AcMu, explores the static behavior of mobile devices, using the regression of the partial least-squares to update the signal map with data from the user's mobile devices. The system uses the signal intensities' readings in real-time received at the reference points to update the model.

In Lim et al. (2010), it is proposed a positioning system that uses signal information among anchor nodes to obtain the exponent of the path-loss model for the environment. This proposal uses the average distance among all anchors to estimate the location. Similarly, the work of Elbakly and Youssef (2016) uses the relative values between pairs of anchors and the site map information, such as walls and obstacles, to decrease the impact of the building infrastructure on the position computation. They evaluate the number of anchors impact on the system performance and the effect of techniques to decrease the signal variation. Their results show an average error of 2.8 m.

An IPS based on signal diversity and least-squares is proposed in Fang and Chen (2020). In the proposed solution, the RSSI noise is first filtered using an adaptive Kalman filter to decrease the variability. Next, the values of two functions are computed using a channel filter to obtain the degree of correspondence between the RSSI values on the different channels to prevent the distance estimation between nodes from falling into local optimum, which would prevent them from reaching the global optimum. The experiments were performed in a small-scale area of 10×10 m^2 with three Bluetooth-based anchors. Their results show an average error of 1.5 m.

Finally, in Paterna et al. (2017), the authors proposed a Bluetooth-based IPSs aimed at improving accuracy while reducing both energy consumption and total cost. The system does not perform signal characterization for the different regions and uses

a static path-loss exponent value. The results show an error of 4.6 m in 90% of the time for a scenario with an area of 16.50 $\times$ 17.60 m². For this, their proposal focused on frequency diversity, signal filtering using the Kalman filter, and a Weighted Least Squares (WLS), without considering the form of anchors organization. The WLS works by increasing the weights of receivers that are closer to the emitter. Their work compares three different propagation models: the International Telecommunication Union (ITU) model, the log-distance model with shadowing, and a fitted empirical model.

In relation to the works that use RSSI, the fingerprint technique is the one that has the best accuracy but is necessary an exhausting training to be implemented. On the other hand, the trilateration technique has a greater error than the fingerprint but is easier to be implemented. In general, the error can be reduced by fixing anchor nodes evenly spaced on 5-meter grids. Table 1 shows a comparison among the works previously described in relation to the techniques used, the IPS scenario size, the number of anchor nodes fixed in the environment, and the average positioning error.

Table 1 – Comparison table among related works.

Author	Techinique	Dimension	Anchors	Error
(Bahl and Padmanabhan, 2000)	WiFi Fingerprint	43 x 22 m	3	2.9 m
(Lim et al., 2010)	WiFi Trilateration	23 x 26 m	8	3.0 m
(Dickinson et al., 2016)	BLE Trilateration	800 m^2	25	2.1 m
(Elbakly and Youssef, 2016)	WiFi Trilateration	26 x 17 m	10	2.8 m
(Paterna et al., 2017)	BLE Trilateration	16 x 17 m	4	4.6 m
(Li et al., 2018)	WiFi Trilateration	9 x 6 m	4	2.2 m
(Wu et al., 2019)	BLE Trilateration	18 x 12 m	25	0.9 m
(Fang and Chen, 2020)	BLE Trilateration	10 x 10 m	3	3.0 m

2.5.1 Discussion

Our proposed PoDME solution differs from all of the mentioned solutions. First, our solution is implemented in large-scale scenarios compared to the scenarios from the previous works, which are implemented in small scenarios, with a high density of anchor nodes, and they use a static path-loss exponent to characterize signal, which is not suitable for large environments. Second, our model-based IPS uses a propagation

model with dynamic path-loss exponent values that allow selecting the best values of the signal loss by distance that characterize the region of the mobile node we want to localize. This results in better accuracies for the estimated distances in large environments, unlike the static parameters for all regions of the environment. Third, we propose a novel method for choosing the best anchor nodes that benefit the least-squares-based position computation by using both the highest RSSI values and the similarity to equilateral triangles, which increases considerably the positioning accuracy compared to approaches that choose anchor nodes only respect to signal strength. The details of our proposed solution are described in the next chapter.

3 PoDME Method

In this chapter, we present our proposed PoDME architecture. Figure 1 shows the components of our system. In the offline phase, we performed model data gathering and obtained the path-loss estimates between the anchor nodes. In the online phase, we perform the position computation using the RSSI values, choosing the best anchor nodes, and using the path-loss estimates obtained in the offline phase to improve the distance mapping between the mobile device and the anchor nodes. All of these components are detailed in the next sections.

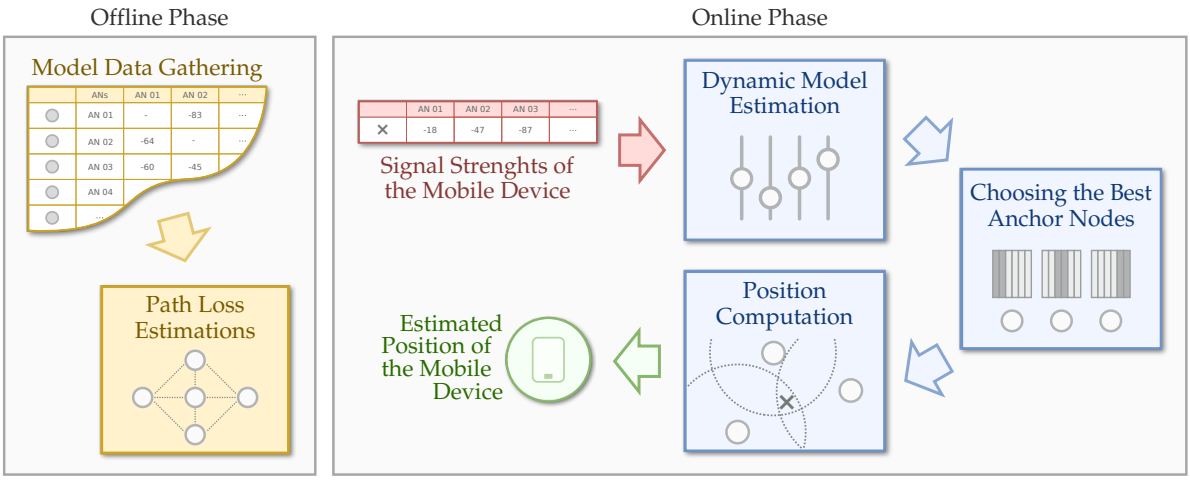

Figure 1 – Phases and components of our PoDME architecture.

3.1 Model Data Gathering

Our solution's first step is to collect some RSSI samples to obtain signal behavior in the environment. Most proposed model-based solutions in the literature require some signal information to fit their models. In some solutions, it is done automatically (Elbakly

and Youssef, 2016; Lim et al., 2010), in others, manually (Li et al., 2018; Sadowski and Spachos, 2018).

Our goal is to create a database containing the RSSI values that represent the distances among anchor nodes and use it to estimate the path-loss exponent in different regions of the environment. We consider that we know the positions of the anchors, which is common in these type of IPS (Fang and Chen, 2020; Huang et al., 2019; Wu et al., 2019; Yong et al., 2020) and, thus, we can quickly obtain the distance among anchors by computing the Euclidean distance, as shown in Equation (3.1).

$$d_{ab} = \sqrt{(x_a - x_b)^2 + (y_a - y_b)^2} \tag{3.1}$$

where d_{ab} is the distance between Anchor$_a$ and Anchor$_b$.

Now we need to know the RSSI behavior among the anchors. Therefore, in this part of our PoDME solution, we propose a simple data gathering methodology in which a person gets one or more mobile devices and physically positions himself below or near an anchor node. From that location, the mobile devices start sending packets. These packets will be received by all nearby anchors with different RSSI values, depending on their positions and the characteristics of the environment in that region. This step is repeated for all anchors in the scenario.

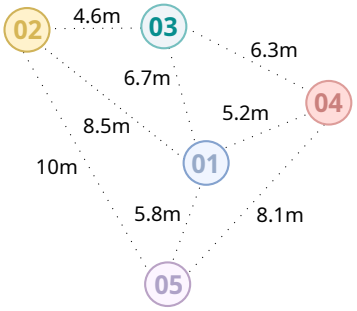

Figure 2 – True distances among anchor nodes obtained through the site plan.

Since we are using Bluetooth advertising packets, we need to filter the RSSI values before using them. Besides the known RSSI variation, the use of Bluetooth advertising packets has another problem: packet loss. It happens because the nodes send these packets in three different channels and, thus, the receiver needs to alternate among these channels constantly. In our experiments, it is common for the anchors to

lose nearly 50% of the packets. To solve this problem, we used the highest RSSI value from the last 1 seconds to smooth out RSSI on each measurement, as the device sends 1 packet every 100 ms, and for small windows, the highest RSSI proved to be better than average value.

Table 2 – RSSI values between anchor nodes. Gathered by physically positioning a mobile node near an anchor node and sending packets that will be received by all other nearby anchors. This step is repeated for all anchor nodes in the scenario.

$\textbf{Anchor}_{neighbor}$	$\textbf{Anchor}_1$	$\textbf{Anchor}_2$	$\textbf{Anchor}_3$	$\textbf{Anchor}_4$	$\textbf{Anchor}_5$
$\textbf{Anchor}_1$	-	-89	-90	-85	-77
$\textbf{Anchor}_2$	-89	-	-75	-	-80
$\textbf{Anchor}_3$	-90	-75	-	-73	-
$\textbf{Anchor}_4$	-85	-	-73	-	-82
$\textbf{Anchor}_5$	-77	-80	-	-82	-

As a result, after taking the measurements, we obtain the RSSI values of all anchors to all of their neighbors. However, since we need only one RSSI value, we take several RSSI samples and use the average RSSI as the value that represents the signal among each anchor node. In Table 2, we have an example of a Model Data Gathering containing the RSSI values between 5 anchors. In the table, not filled cells mean that we have no signal between the two anchors, which indicates that they are far from each other. The relationship between RSSI and distance can be seen in Table 2 and Figure 2. For example, the Anchor_2 is positioned at a distance of 10 m from Anchor_5 and has an RSSI average of -80 dBm. On the other hand, the Anchor_2 is positioned at a shorter distance from Anchor_1, about 8.5 m, and the RSSI value of -89 is weaker when compared to Anchor_1. This is mainly due to more interference caused by obstacles between them. This factor is corrected by the path-loss exponent detailed in the next section.

3.2 Path-Loss Estimations

Now that we have the distances among anchor nodes, given by the map information and Equation (3.1), and also the RSSI values among these anchors, collected in the previous section, we can estimate the best parameters for a Path-Loss Model. Since

there are different distances among anchors and different RSSI values, we will have a different Path-Loss Model for each pair of anchors.

A Path-Loss Model predicts the fading of a signal as it travels a given distance. Such behavior of the signal variation with respect to distance is usually modeled by a logarithmic equation. Several propagation models are proposed in the literature to better relate the signal, distances, and obstacles. However, the Logarithmic Distance Path-Loss Model, described in section 2.3, is the most known and used (Li et al., 2018; Yim, 2012).

Thus, the only environment-dependent variable of the model is the path-loss exponent (η). From Equation (2.1), we can compute this parameter for each pair of anchors:

$$\eta_{ab} = \frac{R_0 - R_{ab}}{10 \times \log_{10} \frac{d_{ab}}{d_0}} \tag{3.2}$$

where η_{ab} is the path-loss exponent between Anchor$_a$ and Anchor$_b$, R_{ab} is the RSSI between them, as shown in Table 2 and, finally, d_{ab} is the distance between them, as in Equation (3.1). Please note that we ignored the parameter X_σ, since R_{ab} is an averaged value from several samples.

Therefore, we can estimate all of the path-loss exponents in the scenario because we know the real position among them and their signals, so we can apply that information to the signal propagation model. A higher η_{ab} would indicate a higher number of obstacles and other fading factors between Anchor$_a$ and Anchor$_b$, while two anchors with direct visibility from each other would result in a lower path-loss exponent. Table 3 show examples of path-loss exponents for the values in Figure 2 and Table 2. It is worth noting how these values change from one anchor node to another. When we establish the path-loss exponent between two anchor nodes, we are characterizing the signal behavior in the region in which they are located, based on their respective positions on the map. Thus, when a mobile device sends a packet and has the signal strengths collected, the distance estimation is made using the respective values of path-loss exponents between the nearest anchors.

Table 3 – Path-loss exponents among anchor nodes calculated through the Equation (3.2) using the RSSI values from the Table 2.

$\textbf{Anchor}_{neighbors}$	$\textbf{Anchor}_1$	$\textbf{Anchor}_2$	$\textbf{Anchor}_3$	$\textbf{Anchor}_4$	$\textbf{Anchor}_5$
$\textbf{Anchor}_1$	-	4.2	4.8	4.9	3.6
$\textbf{Anchor}_2$	4.2	-	3.8	-	3.0
$\textbf{Anchor}_3$	4.8	3.8	-	2.9	-
$\textbf{Anchor}_4$	4.9	-	2.9	-	3.5
$\textbf{Anchor}_5$	3.6	3.0	-	3.5	-

3.3 Choosing the Best Anchor Nodes

The next part of our proposed PoDME solution is executed every time we have a new sample to locate, i.e., a mobile node sent a packet that was received by several anchor nodes, and we need to estimate the mobile position. In this part, we will choose, among all anchors that received the packet, which ones we will use in the next parts of our solution.

The main reason for choosing the best anchors is because the Position Computation part of our solution, detailed in Section 3.5, uses the least-squares technique to find the position of the target. This technique uses distances computed using our Dynamic Model Estimation (detailed in the next section) to find the most consistent position. However, using all of the anchors information, leads to greater errors, since we will use information from faraway anchors, that will have higher distance errors. On the other hand, if we use only the information from the three closest anchors (based on their RSSI values), their positions may be somewhat collinear, which greatly decreases the estimated position accuracy. Thus, in this part, we aim at choosing the closest three anchors that are far from being collinear.

For this, the first step is to sort the list of anchors that received the mobile node packet by their RSSI values in such a way that the closest anchors will be at the beginning of the list. Then, we get the three closest anchors and check their positions against an equilateral triangle similarity filter that will be detailed in the next paragraphs. This test will tell how close the anchors positions form an equilateral triangle since this would be the farthest from them being collinear and, thus, the best-case scenario. If the three closest anchors pass the filter, they will be the chosen anchors for the next parts of our

architecture. However, if the anchors fail the check, i.e., they are somewhat collinear, we ignore them and test the second closest anchors, and so on. If we reach the end of all anchors combinations and they all have failed the similarity checker, we then fall back to the three nearest anchors, considering only the signal strength, as we no longer have other options regarding the organization of the anchor nodes.

Given the positions of three anchors (Anchor_a, Anchor_b, Anchor_c), our equilateral triangle similarity checker starts by computing the internal angles (α, β, γ) of the triangle formed by the anchors positions:

$$\alpha = \left(\frac{\cos {d_{ac}}^2 + {d_{bc}}^2 - {d_{ab}}^2}{2 \times d_{ac} \times d_{bc}} \right) \times 180/\pi \tag{3.3}$$

$$\beta = \left(\frac{\cos {d_{ab}}^2 + {d_{bc}}^2 - {d_{ac}}^2}{2 \times d_{ab} \times d_{bc}} \right) \times 180/\pi \tag{3.4}$$

$$\gamma = \left(\frac{\cos {d_{ab}}^2 + {d_{ac}}^2 - {d_{bc}}^2}{2 \times d_{ab} \times d_{ac}} \right) \times 180/\pi \tag{3.5}$$

Then, we compute how far from $60°$ these angles are since an equilateral triangle has three internal angles of $60°$:

$$\Delta = \sqrt{(\alpha - 60)^2 + (\beta - 60)^2 + (\gamma - 60)^2} \tag{3.6}$$

The closer Δ is from zero, the closer the anchors are to form an equilateral triangle. The threshold chosen in our proposed solution has a value of 75. Thus, if the three anchors at the beginning of the list have a Δ between zero and 75, then they can be used in the position calculation, otherwise, we evaluate other sets. This threshold was obtained empirically, as will be shown in our performance evaluation in Section 4.

3.4 Dynamic Model Estimation

As shown in Section 3.2, the only environment-dependent variable of the log-distance model is the path-loss exponent (η). As mentioned, in most model-based IPSs (Fang and Chen, 2020; Paterna et al., 2017; Shi et al., 2017; Teoman and Ovatman, 2019) this

parameter is static for the whole scenario. Static path-loss exponent is not recommended for large-scale scenarios since the path-loss exponent changes from place to place depending on the obstacles and other environment variables. In our PoDME solution, we propose the use of a dynamically computed path-loss exponent, in such a way that this value corresponds more closely to the characteristics of the region the packet we want to localize was sent from.

In the last section, we chose the best three anchors to be used to locate that specific packet sent by the mobile node. These anchors are closer to the mobile node and, thus, their information can be used to estimate the local path-loss exponent to be used in the position computation. The goal is to use the average value of the path-loss exponent among the neighbors anchors to represent the region where the mobile device is located. For this, we use the path-loss estimations, computed in Section 3.2. There, we computed the path-loss exponent among all pairs of anchors. Since in the next section, we will need three distance estimations, one for each anchor, we will compute three different path-loss exponents. Thus, the final path-loss exponent, for a given anchor, will be the average exponent between this anchor and the other two:

$$\eta_{ma} = (\eta_{ab} + \eta_{ac})/2 \tag{3.7}$$

$$\eta_{mb} = (\eta_{ba} + \eta_{bc})/2 \tag{3.8}$$

$$\eta_{mc} = (\eta_{ca} + \eta_{cb})/2 \tag{3.9}$$

where η_{ma} is the path-loss exponent that will be used to compute the distance between the mobile node and Anchor$_a$, and so on.

As we can see, the model parameters estimated in this part of PoDME depend mainly on the anchors that heard the packet from the mobile node. Thus, this parameter can change for each packet sent by the mobile node, depending on its location. In the next section, we will use these parameters to, finally, compute the node's position.

3.5 Position Computation

Now that we have the path-loss model for the three best anchor nodes, we can convert the RSSI value of the packet sent by the mobile node and received by the anchors through an adaptation of Equation (2.1):

$$d_{ma} = 10^{\left(\frac{R_0 - R_{ma}}{10 \times \eta_{ma}}\right)}; \qquad d_{mb} = 10^{\left(\frac{R_0 - R_{mb}}{10 \times \eta_{mb}}\right)}; \qquad d_{mc} = 10^{\left(\frac{R_0 - R_{mc}}{10 \times \eta_{mc}}\right)} \tag{3.10}$$

where d_{ma} is the estimated distance between the mobile node and the Anchor$_a$, and so on.

Since the real positions of the anchors are known in advance and the distances are estimated using the previous equations, we can finally compute the mobile node position. For this, each anchor will have a circle of radius equal to the estimated distance, and the final target position will correspond to the intersection of the three circles. However, since we will have inaccuracies in our distance estimations, due to the RSSI variation (Wu et al., 2019), the formed circles often do not have a single intersection. To minimize this problem, we use the least-squares method (Wu et al., 2019; Xia et al., 2019) to optimize the position computation, as follow:

$$f_i(x, y) = d_{mi} - \sqrt{(x_m - x_i)^2 + (y_m - y_i)^2} \tag{3.11}$$

$$min(x, y) = min \sum_{i=1}^{m} [f_i(x, y)]^2, \quad m \geq 3 \tag{3.12}$$

However, it is difficult to resolve directly. To simplify, we can define the Equation (3.11) as $fi(x_m, y_m) = 0$ and squared both sides to obtain:

$${x_m}^2 + {y_m}^2 - 2x_m x_i - 2y_m y_i = {d_{mi}}^2 - {x_i}^2 - {y_i}^2 \tag{3.13}$$

Given the three anchors (Anchor$_a$, Anchor$_b$, Anchor$_c$), their coordinates (x_a, y_a), (x_b, y_b), and (x_c, y_c), and the coordinate of mobile device (x_m, y_m). Then, if we set

$w = {x_m}^2 + {y_m}^2$, we can organize as follows:

$$\begin{cases} w - 2x_m x_a - 2y_m y_a = {d_{ma}}^2 - {x_a}^2 - {y_a}^2 \\ w - 2x_m x_b - 2y_m y_b = {d_{mb}}^2 - {x_b}^2 - {y_b}^2 \\ w - 2x_m x_c - 2y_m y_c = {d_{mc}}^2 - {x_c}^2 - {y_c}^2 \end{cases} \tag{3.14}$$

Then we can obtain an equation of the form $AX = b$:

$$A = \begin{bmatrix} 1 & -2x_a & -2y_a \\ 1 & -2x_b & -2y_b \\ 1 & -2x_c & -2y_c \end{bmatrix}; \quad X = \begin{bmatrix} w \\ x_m \\ y_m \end{bmatrix}; \quad b = \begin{bmatrix} {d_{ma}}^2 - {x_a}^2 - {y_a}^2 \\ {d_{mb}}^2 - {x_b}^2 - {y_b}^2 \\ {d_{mc}}^2 - {x_c}^2 - {y_c}^2 \end{bmatrix} \tag{3.15}$$

Finally, the equation can be solved as a least-squares problem:

$$X = (A^T A)^{-1} A^T b \tag{3.16}$$

The result of the least-squares equation is the mobile node estimated position.

3.5.1 Discussion

Our PoDME solution requires minimal training to obtain the path-loss exponent among the anchor nodes. As the anchor nodes are usually fixed to the environment ceiling, we chose to do the training used a device under each anchor to better represent the communication among them, since the user will always be under the anchors.

In the training phase, it is necessary to create a database that contains the RSSI values among the anchor nodes. Thus, for each anchor node, a collection of 120 signal samples lasting 2 minutes is archived. As the devices are configured to send BLE packets every 100 ms, and it is known that the signal variation is high, so to minimize this variation, each signal sample corresponds to the most strong RSSI sent in the 1 second interval.

On the other hand, we only need an RSSI value to represent the communication between two anchors, as represented in Table 2. Thus, as the training base contains 120 signal samples between neighboring anchors, our solution uses the average of 120

values to obtain the RSSI that represents communication between two anchors, as it was the approach that was most representative in relation to the median, mode, and strong signal.

This approach is also subject to changes in the environment, as new obstacles added to the scenario would change the signal behavior. However, as this step is easy to be performed, the cost is much lower when compared to the fingerprint technique that would require a more exhaustive training phase. Contrary to the need to carry out training by collecting signal values at various points in the environment, usually spaced by 2 meters, our solution requires only N collections, where N is the number of anchor nodes in the scenario. Through the signal representation table among the anchor nodes, the path-loss exponent can be estimated more correctly and thus enable a signal estimate for a more realistic distance.

4 Performance Evaluation

In this chapter, we evaluate the performance of our proposed PoDME solution compared to the traditional static, model-based approaches found in the literature. We also evaluate other aspects of our solution such as the variation of the path-loss exponent in a real-world scenario and the behavior of the data used for choosing the best anchors.

4.1 Methods Comparison

We compared our PoDME solution to three variations of a static model-based IPS. These variations use the log-distance path-loss propagation model, the same used in our solution, but instead of using a dynamic path-loss exponent (η), they use a static value for all scenarios. It is important to note that the exponent value was computed based on the collected RSSI samples and we confirmed that it was the best possible static exponent, i.e., the one that resulted in the smallest errors. Finally, the main difference between these three variations and our solution is the choice of the anchors used for the position computation. While in our solution we used our method explained in Section 3.3, in the models variations we used other possible solutions found in the literature:

1. Using 3 anchors with the highest RSSI values
2. Using 4 anchors with the highest RSSI values
3. Using all anchors

Using 3 (Huang et al., 2019; Sadowski and Spachos, 2018; Yong et al., 2020) or all anchor nodes (Fang et al., 2015; Paterna et al., 2017; Wang et al., 2013) in the position

computation is a solution commonly found in the literature. However, the main reason we also experimented using the 4 anchors with the highest RSSIs, is that it could be a simple solution for the problem of anchors with collinear positions. Thus, as we will see, it resulted in considerably better performance when compared to using only 3 anchors.

4.2 Testbed and Methodology

The main goal of our proposed IPS is to provide location information for small, battery-powered devices to be used by people inside buildings, such as the elderly in retirement homes. These mobile devices are required to be operated by a single, small battery while also having other sensors. Thus, in our IPS, we decided to use the Bluetooth Low Energy (BLE) technology.

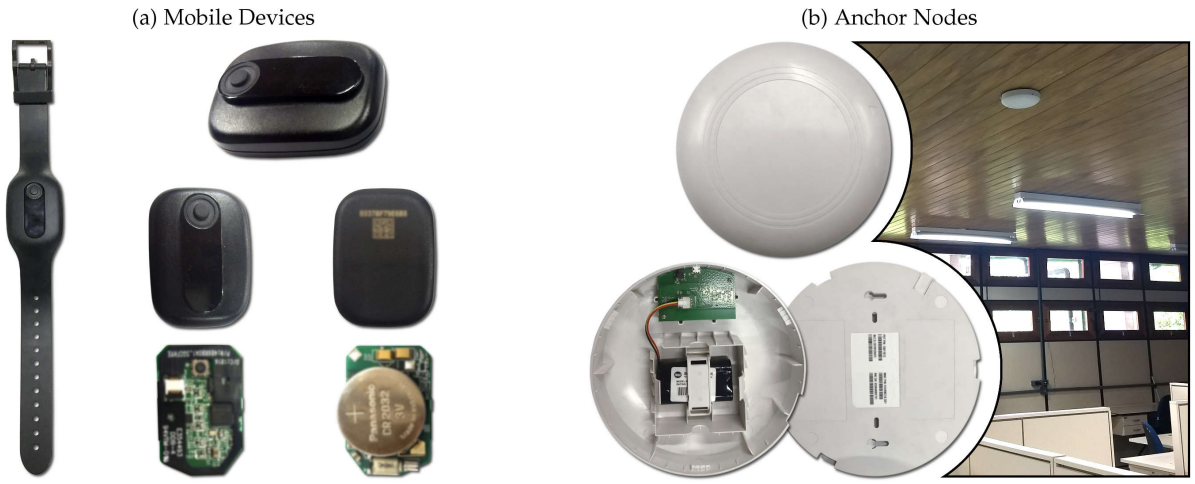

Figure 3 – Testbed hardware: (**a**) mobile devices with Bluetooth communication; and (**b**) anchor nodes with Bluetooth and 900 Mhz communication (front, opened, back, and installed on the ceiling).

Furthermore, one of the premises of the hardware architecture was not to rely on the WiFi infrastructure of the building. Thus, to be able to send all of the gathered RSSI data to a central monitoring server, we developed a Bluetooth-based anchor. The testbed architecture works by mobile devices sending Bluetooth advertising packets every second and several anchors receive these packets. In our experiments, the longest communication distance between Bluetooth devices was 25 m. These anchor nodes compute the RSSI of the received packets by Bluetooth and send them to a central device

using long-range, 900 Mhz communication. The central device is connected to a server, which will locate the mobile nodes. Figure 3 shows our developed hardware that was used in the testbed.

To evaluate the performance of our proposed IPS solution, we carried out a large-scale experiment in a 43 $\times$ 15 m^2 area composed of 15 spaces (11 rooms and 3 halls), as shown in Figure 4. To cover the whole area, we deployed 15 anchor nodes fixed on the ceiling of the rooms in locations where it was somewhat convenient to connect them to the mains supply. It is important to note that to perform our Model Data Gathering, explained in Section 3.1, we used 8 different mobile devices and collected samples at 15 different locations. This was done to estimate the path-loss exponents among anchors with a variety of signals from different devices.

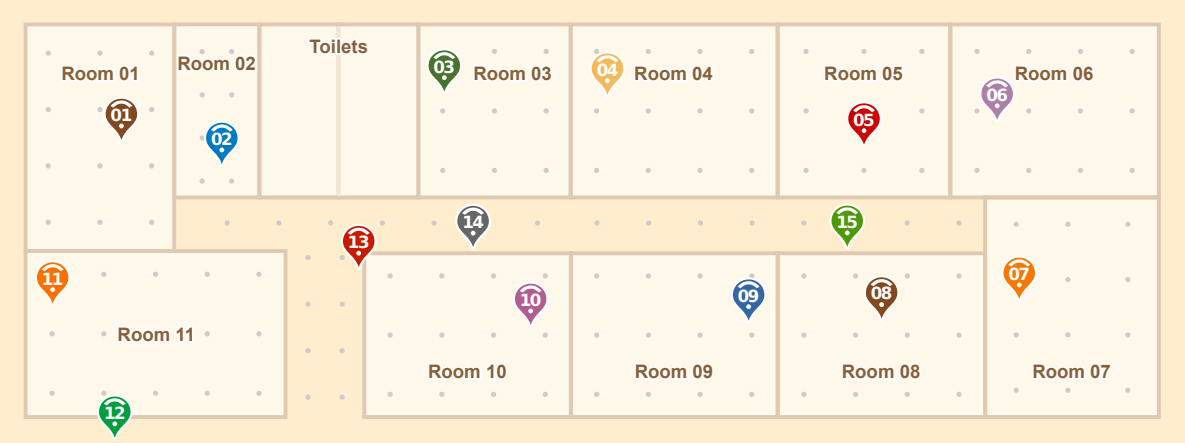

Figure 4 – Testbed map: 11 rooms, 3 halls, and 15 anchor nodes. 100 packet samples collected from 150 test points. The gray points are the test points.

However, to understand and evaluate our system results for the whole scenario, we gathered 100 packet samples from evenly spaced, 2 m apart locations, to a total of 150 different test points, which are the gray dots in Figure 4. For this, we used another three mobile devices that were different from the ones used in the Model Data Gathering. Thus, our testing was done with samples from a set of mobile devices that were not part of the Model Data Gathering. This step is important to ensure that the proposed system would work on new, never seen, mobile devices. Finally, it is important to note that these 150 test points data are not required for our PoDME solution, and were only used for performance evaluation purposes.

4.3 Signal Strength Analysis

To better understand the signal propagation behavior in our testbed environment, Figure 5 shows, for each test point, which anchor nodes received the packets from that point and at which signal strengths. For this, each anchor was given a different color. The stronger the color, the higher the signal strength. This map shows which points are covered by which anchors, and also gives us some insights into the behavior of the IPS. As we will see in the next sections, the lightest points did result in higher errors.

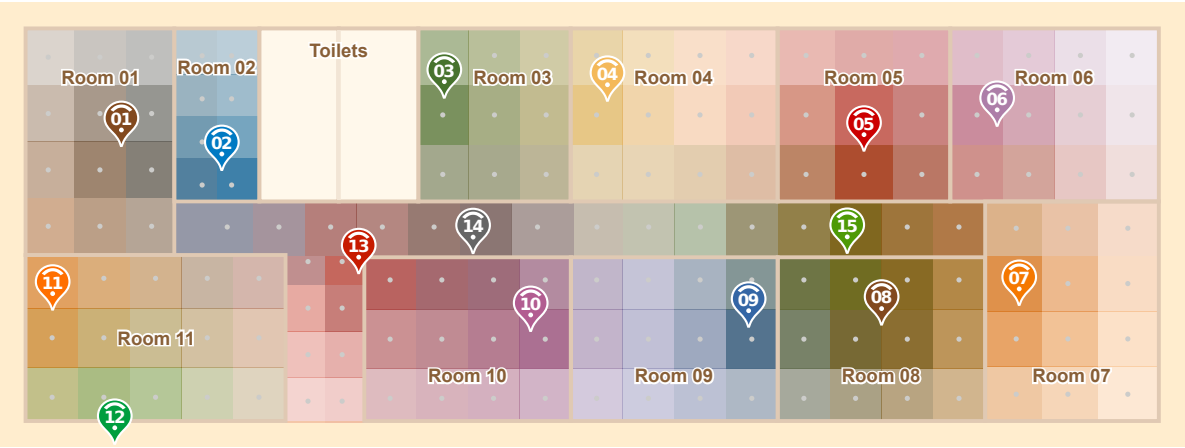

Figure 5 – Signal characterization of the scenario based on the measurements made empirically.

We then used these RSSI data to estimate the path-loss exponent parameter of log-distance propagation model. Our main goal is to allow the visualization of how a propagation model would compare to our real-world data. Thus, we implemented a simple signal propagation simulator. Figure 6 show the result of our simulation. It is interesting to see that, comparing both maps, we can notice that, in most parts, the colors seem to match. Even though this result is not scientific, it will help us to understand some of our obtained results in the next sections.

Figure 6 – Signal characterization of the environment using the signal propagation model.

4.4 Path-loss Exponent Analysis

One of the key points of our PoDME solution is that the path-loss model parameters change throughout the environment and, thus, using a static model would result in higher positioning errors. To depict these changes, Figure 7 shows some of the path-loss exponents among the anchor nodes, as explained in Section 3.2, and based on the anchors of the map in Figure 4. It is important to note that the lines in this figure are just a small subset of the connectivity among anchors and does not represent the full connectivity.

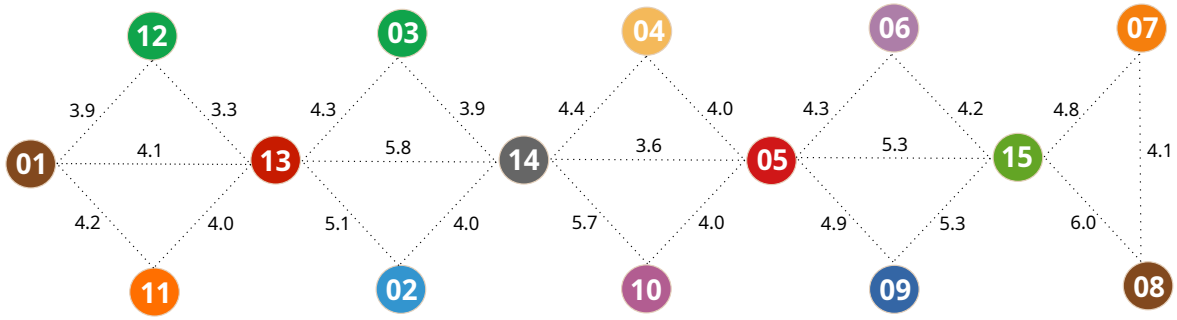

Figure 7 – Path-loss exponents among anchors computed from a real-world experiment. The lines are just a small subset of the connectivity among anchors and does not represent the full connectivity.

As we can see, these values change considerably even among the neighbors of the same anchor. Even though this is a small set of the path-loss exponents, we can see some cases in which the scenario affects the model parameters. For instance, focusing on

$Anchor_3$, we can see that its path-loss exponent to $Anchor_{14}$ is 3.9, while the exponent between $Anchor_3$ and $Anchor_{13}$ is higher, at 4.3. Both $Anchor_{14}$ and $Anchor_{13}$ are at similar distances from $Anchor_3$, the main difference being that $Anchor_{13}$ is shadowed by a corner and also by an extra wall, resulting in a higher path-loss exponent.

4.5 Choosing the Best Anchors Parameters

Our main parameter for choosing the best anchor nodes is the RSSI values, as explained in Section 3.3. Anchors with higher RSSI values are closer to the mobile device, which leads to lower distance estimation errors due to the model inaccuracies (Wu et al., 2019). To better understand the impact of the choice based on this criterion, for each sample to be located in our experiment, we computed the device's position using all possible combinations of 3 anchors. For each computed position, we saved the positioning error and the average RSSI value among the three used anchors.

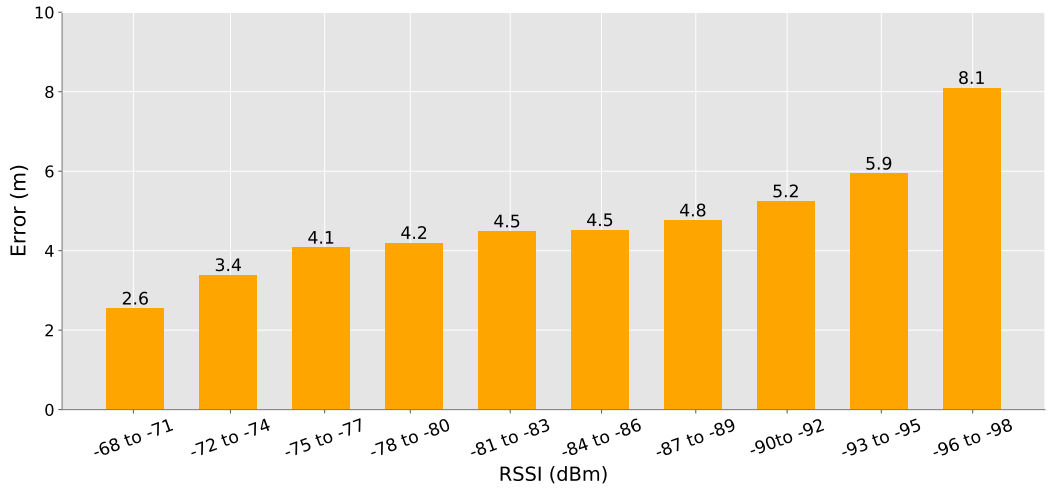

Figure 8 – Positioning error by average RSSI. The farther the anchor nodes, the higher the positioning error. Even slightly farther anchor nodes can increase the positioning error by almost 1 m.

Figure 8 shows our results from the experiment. As expected, anchors with the highest RSSI values have the lowest average positioning error. However, one interesting aspect that we noticed after analyzing the graph, is that the difference between the first and the second bars are higher than expected. It means that getting slightly farther anchors can increase the positioning error by almost 1 m. It does show that our priority

should be using the closest anchors.

Another key aspect of Choosing the Best Anchors is the equilateral triangle similarity checker, the Δ shown in Equation (3.6). As mentioned, we noticed that even for closer anchors, when their positions were somewhat collinear, it resulted in considerably higher errors. Again, to better understand the impact of the anchors choice based on this criterion, for each sample to be located in our experiment, we computed the device's position using all possible combinations of 3 anchors. For each computed position, we saved the positioning error and our equilateral triangle similarity (Δ).

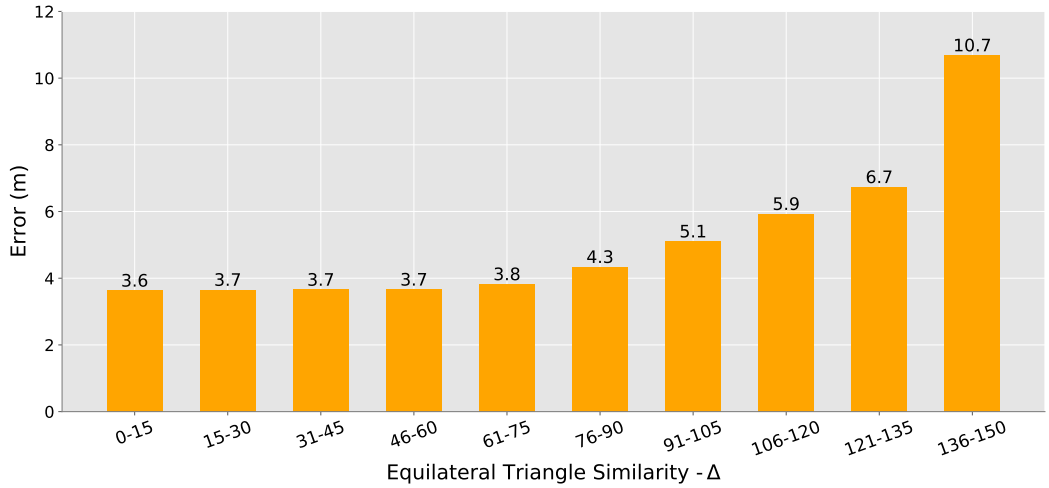

Figure 9 – Positioning error by equilateral triangle similarity. The closer Δ is from zero, the closer the anchor nodes are to form an equilateral triangle. For Δ between 0 and 75, the error does not change significantly.

As shown in Figure 9, we can see that for Δ between 0 and 75, we have an average error that does not change significantly, always below 4 m. However, after this value, the greater the Δ, the greater the average error. After analyzing these experiments and conduct some tests, we observed that combining these two criteria (RSSI and Δ) would not yield the best results, since they have different behaviors. Thus, we decided to use the Δ value as a filter and established a threshold of 75 for allowing a set of three anchors to be used in the positioning while prioritizing the closest anchors.

4.6 Positioning Error Analysis

As mentioned, for our experiment, we captured RSSI samples in all of the points of the scenario to allow a fair comparison of the evaluated methods. For all measurements, we saved their correct positions on the map where the measurement was made, thus allowing us to compare the position estimated by the models and the actual point position.

We first evaluate the average positioning error for each of the methods. As shown in Figure 10a, PoDME resulted in an average error of 3 m, being the smallest error when compared to the other approaches. As mentioned, we used a static path-loss exponent for the model variations. In these cases, the value was $\eta = 4.2$, obtained through the gathered data. Our solution used the dynamic path-loss exponents values chosen based on the region of the three anchors with the highest RSSI values.

The worst results were obtained by the static, model-based method using information from 3 anchors with the highest RSSI values. As mentioned, in some cases, the chosen anchors are located in such a way that make their positions somewhat collinear, increasing considerably the error of the position estimations. As we can also see in Figure 10a, when we consider just one more anchor in the position computation we have a reduction of more than half of the error.

Figure 10b shows the average room accuracy. The room accuracy evaluation was done comparing whether the position estimated by each method was within the room limits where the measurement was performed. Since all of the models do not take into consideration the walls of the scenario, it is common for test points near walls to be located outside their rooms. Furthermore, small regions such as halls, also impact this metric, since the positioning error is greater than their width. However, as shown in Figure 10b, our proposal resulted in a greater room accuracy of 74.8%. As we will discuss in our conclusions, in our future work we intend to use a model that also takes into consideration the walls of the area, aiming at improving this metric.

The results obtained by our solution show that contrary to what it may seem initially if we continue using only 3 anchors, but considering better criteria for choosing these anchors, we can considerably reduce the total average error of the system. In

Figure 10c, the curve of our solution (red line) grew the fastest. This means that our results contain the highest number of mobile devices with the smallest positioning error when compared to the other approaches. In Figure 10d, we can see that our approach contains most of the positioning errors between 0-4 m, although part of the samples was still located with higher errors. This happens due to regions of the map that are covered by only 3 anchors, not allowing the choice of other sets that could help in reducing the positioning error.

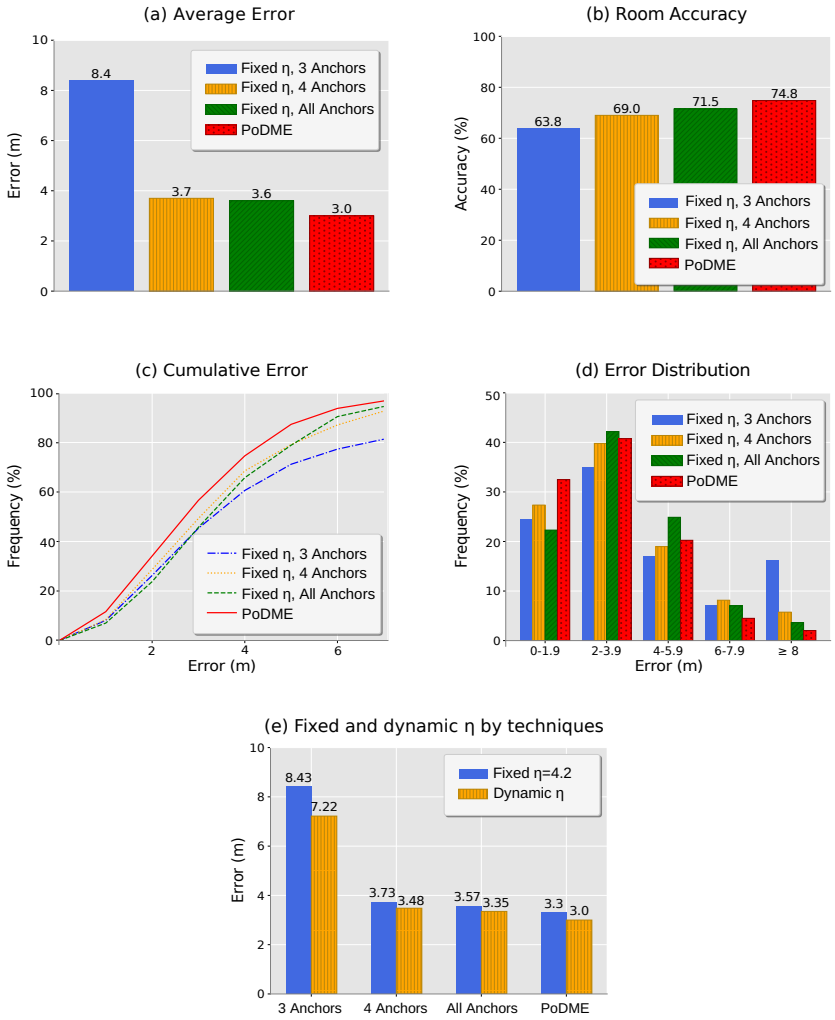

Figure 10 – Positioning error analysis.

To evaluate the impact of the value used as the path-loss exponent, in Figure 10e, we can see the average positioning error in relation to the use of a static path-loss exponent value or the use of our proposed dynamic value. These results show that our proposed dynamic model was able to improve the accuracy of all evaluated variations of anchor choice. We can also see that our proposed PoDME solution takes advantage of

Room	**3 Anchors**		**4 Anchors**		**All Anchors**		**PoDME**
	Static	Dynamic	Static	Dynamic	Static	Dynamic	
Room 01	3.96	3.11	3.70	3.10	3.72	3.10	3.12
Room 02	3.30	2.86	3.90	3.07	3.90	3.07	3.00
Room 03	2.54	2.64	3.46	2.77	4.02	3.01	2.64
Room 04	48.52	35.21	6.27	5.50	3.59	3.98	3.67
Room 05	3.47	3.06	3.26	2.97	3.54	3.37	3.00
Room 06	3.58	4.31	3.13	4.13	4.29	4.13	4.32
Room 07	3.86	4.63	3.34	4.42	2.75	4.21	4.29
Room 08	2.77	3.16	2.38	2.49	3.07	2.61	2.39
Room 09	5.88	6.21	3.87	3.82	2.60	2.63	2.60
Room 10	4.51	3.35	3.90	2.89	3.23	2.58	2.70
Room 11	2.76	2.37	3.20	2.86	3.20	3.56	2.24
Hallway 1	7.24	8.47	3.38	3.45	4.49	3.92	3.39
Hallway 2	3.25	2.73	2.22	2.02	3.34	2.18	2.23
Hallway 3	5.5	7.43	6.02	4.37	5.69	4.32	3.86
Average	$8.43m$	$7.22m$	$3.73m$	$3.48m$	$3.57m$	$3.35m$	$3.00m$

Table 4 – Table with average error per room comparing the different approaches.

not only the dynamic model but also the anchors choice, i.e., both aspects are responsible for improving the accuracy of the solution.

To better understand the behavior of the errors throughout the evaluated scenario, Table 4 shows the average error obtained by each approach for all rooms in the environment. We can see that the smallest errors per room vary a lot according to the approach used, that is, each room has its smallest error with different approaches. When we use 3 anchors, most measurements in Room 04 have the anchor nodes 3, 4, and 5 with the strongest signal power values. In this case, their organization on the map results in a high positioning error, as can be seen in Table 4. When we add an additional anchor node, the positioning error is drastically reduced. In our solution, even using only three anchors we obtain a low error as we choose the best anchors that help in the positioning calculation.

In most cases, our PoDME solution resulted in positioning errors close enough to the smallest error between all approaches. We use values in bold to facilitate comparison. The rooms with higher errors were rooms 06 and 07, on the right side of the map. The main reason for this is the lack of anchors coverage in some areas of these rooms, as depicted previously in Figure 6.

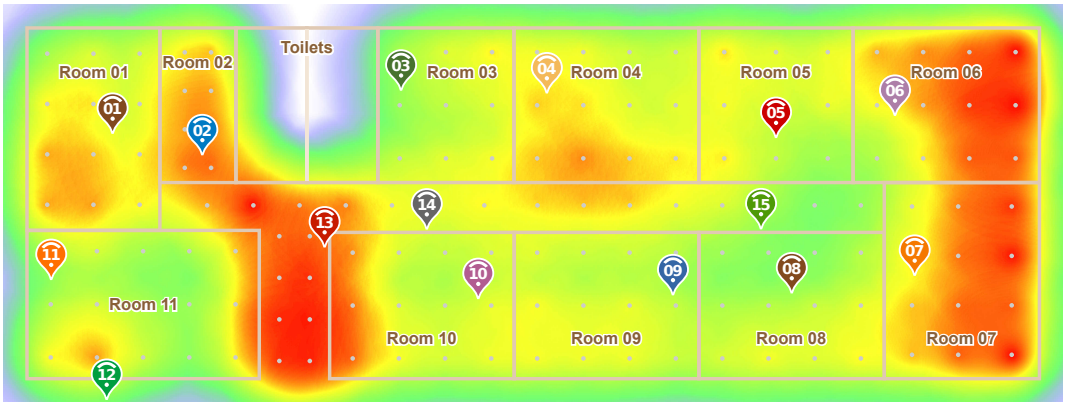

Figure 11 – Heatmap of the average errors for each test point in the scenario, showing the best positioning regions.

Finally, in order to better visualize the data in Table 4, Figure 11 shows a heatmap of the errors in the whole scenario. Darker red colors indicate the areas with the highest errors. In this heatmap, we can notice another problematic region of the scenario, which is the hall near Anchor_{13}. In this area, especially towards the bottom of the map, the other anchors (besides 13), are far from the hall which, combined with the walls in the area, resulted in a worse performance. This lack of anchors coverage can also be noticed in Figure 6.

5 Conclusions

In this work, we propose and evaluate a new model-based IPS, in which the parameters of the model are dynamically estimated using the RSSI information from the best anchor nodes that received the packet sent by the mobile device we want to locate. Thus, for each packet sent by the mobile device, depending on its location, we have a different propagation model that will be used to estimate distances and, then, positions. The main goal of our proposed solution is to be implemented in medium to large-scale scenarios, in which a fingerprint-based solution would be hard or unfeasible to train and, also, a static, model-based solution would result in higher errors due to the static parameters of the model for the whole scenario. We also aim at applications in which mobile devices are highly energy-efficient such as small, battery-powered, sensor-based smartwatches, to be easily worn by people inside buildings such as the elderly in retirement homes.

Thus, we implemented a complete large-scale, Bluetooth-based testbed using custom-made hardware to evaluate the performance of our solution and compare it to traditional static, model-based solutions used by the current literature. Our experiments show a significant contribution in two of the main parts of our solution: the best anchors choice algorithm and the dynamic model estimation. When combined, our preliminar solution resulted in an average error of 3 m, a 17% decrease when compared to the best experimented parameter of a static model-based IPS, that had an error of 3.6 m.

5.1 Limitations And Future Work

It is known that fingerprint-based solutions are among the most precise solutions for IPSs (Bahl and Padmanabhan, 2000; Honkavirta et al., 2009; Youssef and Agrawala,

2005; Yu-liang, 2013). However, they require an extensive training phase, making them basically impractical for medium to large-scale settings. One can argue that our proposed PoDME solution also has a training phase, which would be Model Data Gathering (explained in Section 3.1). However, in our solution, we do not train all possible reference points of the environment but, rather, only a single point for each anchor. As a comparison, in the experiments explained in Section 4 and depicted in Figure 4, we only needed to collect some samples from 15 different locations to generate our model. This can be done in fewer than 15 minutes since it does not require many samples. For a fingerprint-based solution, it would be required to train at least all of the 150 tested locations in our experiments. It took us several days to have unimpeded access to the rooms and collect enough data from all the points. Also, the number of reference points increases drastically as the scenario increases.

Also, our Model Data Gathering could be done automatically by the anchors, by modifying them to send data packets among themselves, as done by some works in the literature (Elbakly and Youssef, 2016; Lim et al., 2010). However, we do not think that this would be the best solution, since the signal strengths from packets exchanged between the anchors, which are all located in the ceiling, would differ significantly from the packets sent by the mobile nodes, which would be located in a mid-height. The main reason for this is the interference caused by the ceiling itself. Thus, we argue that our proposed Model Data Gathering would yield the best results, with little to no extra work when compared to other model-based IPSs.

Even though we used the log-distance propagation model, our solution can also be applied to any other propagation model. As next steps, we intend to experiment mainly with models that take into consideration the walls of the scenario. We also aim at proposing better algorithms for choosing the best anchor nodes by also taking advantage of the walls' information. Finally, we will perform additional experiments to propose better solutions for the tested points located in small rooms, halls, and areas with less anchors coverage, since these were the areas that resulted in greater positioning errors and lower room accuracies.

Bibliography

Al Kalaa, M. O. and Refai, H. H. (2015). Selection probability of data channels in bluetooth low energy. In *2015 International Wireless Communications and Mobile Computing Conference (IWCMC)*, pages 148–152. pages 5

Bahl, P. and Padmanabhan, V. N. (2000). Radar: an in-building rf-based user location and tracking system. In *Proceedings IEEE INFOCOM 2000. Conference on Computer Communications. Nineteenth Annual Joint Conference of the IEEE Computer and Communications Societies (Cat. No.00CH37064)*, volume 2, pages 775–784 vol.2. pages 10

Bahl, V. and Padmanabhan, V. (2000). Enhancements to the RADAR User Location and Tracking System. *Microsoft Research*, 2(MSR-TR-2000-12):775–784. pages 12, 35

Brena, R., García-Vázquez, J., Galván Tejada, C., Munoz, D., Vargas-Rosales, C., Fangmeyer Jr, J., and Palma, A. (2017). Evolution of indoor positioning technologies: A survey. *Journal of Sensors*, 2017. pages 1, 7

Chan, S. and Sohn, G. (2012). Indoor localization using wi-fi based fingerprint and trilateration techiques for lbs applications. *ISPRS - International Archives of the Photogrammetry, Remote Sensing and Spatial Information Sciences*, XXXVIII-4/C26:1–5. pages 7

Dickinson, P., Cielniak, G., Szymanezyk, O., and Mannion, M. (2016). Indoor positioning of shoppers using a network of bluetooth low energy beacons. In *2016 International Conference on Indoor Positioning and Indoor Navigation (IPIN)*, pages 1–8. pages 5, 8, 10, 12

Elbakly, R. and Youssef, M. (2016). A robust zero-calibration rf-based localization system for realistic environments. In *2016 13th Annual IEEE International Conference on Sensing, Communication, and Networking (SECON)*, pages 1–9. pages 11, 12, 14, 36

Fang, S.-H., Hsu, Y.-T., Shiao, Y., and Sung, F.-Y. (2015). An enhanced device localization

approach using mutual signal strength in cellular networks. *IEEE Internet of Things Journal*, 2:1–1. pages 24

Fang, X. and Chen, L. (2020). An optimal multi-channel trilateration localization algorithm by radio-multipath multi-objective evolution in rss-ranging-based wireless sensor networks. *Sensors*, 20:1798. pages 2, 11, 12, 15, 19

Faragher, R. and Harle, R. (2015). Location fingerprinting with bluetooth low energy beacons. *IEEE Journal on Selected Areas in Communications*, 33:1–1. pages 2, 9

Glitza, J., Zhang, P., Abdelaal, M., and Theel, O. (2017). An improved ble indoor localization with kalman-based fusion: An experimental study. *Sensors*, 17:951. pages 6

He, S. and Chan, S. . G. (2016). Wi-fi fingerprint-based indoor positioning: Recent advances and comparisons. *IEEE Communications Surveys Tutorials*, 18(1):466–490. pages 2, 9

Honkavirta, V., Perala, T., Ali-Loytty, S., and Piche, R. (2009). A comparative survey of WLAN location fingerprinting methods. In *Navigation and Communication 2009 6th Workshop on Positioning*, pages 243–251. pages 35

Huang, k., He, K., and Du, X. (2019). A hybrid method to improve the ble-based indoor positioning in a dense bluetooth environment. *Sensors*, 19:424. pages 7, 15, 24

Ji, Y., Biaz, S., Pandey, S., and Agrawal, P. (2006). Ariadne: a dynamic indoor signal map construction and localization system. In *MobiSys '06*. pages 9

Li, G., Geng, E., Ye, Z., Xu, Y., Lin, J., and Pang, Y. (2018). Indoor positioning algorithm based on the improved rssi distance model. *Sensors*, 18:2820. pages 1, 2, 10, 12, 15, 17

Lim, C., Wan, Y., Ng, B., and See, C. S. (2007). A real-time indoor wifi localization system utilizing smart antennas. *IEEE Transactions on Consumer Electronics*, 53(2):618–622. pages 8

Lim, H., Kung, L.-C., Hou, J. C., and Luo, H. (2010). Zero-configuration indoor localization over ieee 802.11 wireless infrastructure. *Wirel. Netw.*, 16(2):405–420. pages 11, 12, 15, 36

Liu, H., Chen, W., and Hsu, P. (2019). Comparison of nva and rlowess algorithms in indoor positioning system. In *2019 20th Asia-Pacific Network Operations and Management Symposium (APNOMS)*, pages 1–4. pages 6

Liu, H., Darabi, H., Banerjee, P., and Liu, J. (2007). Survey of wireless indoor positioning

techniques and systems. *IEEE Transactions on Systems, Man, and Cybernetics, Part C (Applications and Reviews)*, 37(6):1067–1080. pages 8

Luo, J. and Zhan, X. (2014). Characterization of smart phone received signal strength indication for wlan indoor positioning accuracy improvement. *J. Networks*, 9:739–746. pages 6

Ni, W., Shen, G., Leng, X., and Gui, L. (2006). An indoor location algorithm based on taylor series expansion and maximum likelihood estimation. In *2006 IEEE 17th International Symposium on Personal, Indoor and Mobile Radio Communications*, pages 1–4. pages 1, 10

Onofre, S., Silvestre, P. M., Pimentão, J. P., and Sousa, P. (2016). Surpassing bluetooth low energy limitations on distance determination. In *2016 IEEE International Power Electronics and Motion Control Conference (PEMC)*, pages 843–847. pages 5, 10

Paterna, V., Calveras, A., Aspas, J., and Bullones, M. (2017). A bluetooth low energy indoor positioning system with channel diversity, weighted trilateration and kalman filtering. *Sensors*, 17:2927. pages 5, 11, 12, 19, 24

Sadowski, S. and Spachos, P. (2018). Rssi-based indoor localization with the internet of things. *IEEE Access*, 6:30149–30161. pages 1, 6, 15, 24

Shi, Y., Long, Y., Lu, F., Xu, Z., Xiao, X., and Shi, S. (2017). Indoor rssi trilateral algorithm considering piecewise and space-scene. In *2017 IEEE International Conference on Smart Cloud (SmartCloud)*, pages 278–282. pages 2, 10, 19

Sung, Y. (2016). Rssi-based distance estimation framework using a kalman filter for sustainable indoor computing environments. *Sustainability*, 8:1136. pages 6

Tariq, Z. B., Cheema, D. M., Kamran, M. Z., and Naqvi, I. H. (2017). Non-gps positioning systems: A survey. *ACM Comput. Surv.*, 50(4). pages 7, 8

Teoman, E. and Ovatman, T. (2019). Trilateration in indoor positioning with an uncertain reference point. In *2019 IEEE 16th International Conference on Networking, Sensing and Control (ICNSC)*, pages 397–402. pages 2, 19

Torteeka, P. and Chundi, X. (2014). Indoor positioning based on wi-fi fingerprint technique using fuzzy k-nearest neighbor. In *Proceedings of 2014 11th International Bhurban Conference on Applied Sciences Technology (IBCAST) Islamabad, Pakistan, 14th - 18th January, 2014*, pages 461–465. pages 2

Wang, Y., Xu Yang, Yutian Zhao, Yue Liu, and Cuthbert, L. (2013). Bluetooth positioning using rssi and triangulation methods. In *2013 IEEE 10th Consumer Communications*

and Networking Conference (CCNC), pages 837–842. pages 24

Wu, C., Yang, Z., and Xiao, C. (2018). Automatic radio map adaptation for indoor localization using smartphones. *IEEE Transactions on Mobile Computing*, 17(3):517–528. pages 11

Wu, T., Xia, H., Liu, S., and Qiao, Y. (2019). Probability-based indoor positioning algorithm using ibeacons. *Sensors*, 19:5226. pages 2, 10, 12, 15, 21, 29

Xia, H., Zuo, J., Liu, S., and Qiao, Y. (2019). Indoor localization on smartphones using built-in sensors and map constraints. *IEEE Transactions on Instrumentation and Measurement*, 68(4):1189–1198. pages 21

Yim, J. (2012). Comparison between rssi-based and tof-based indoor positioning methods. *International Journal of Multimedia and Ubiquitous Engineering*, 7. pages 17

Yong, S., Shi, W., Liu, X., and Xiao, X. (2020). An rssi classification and tracing algorithm to improve trilateration-based positioning. *Sensors (Basel, Switzerland)*, 20:4244. pages 2, 7, 9, 15, 24

Youssef, M. and Agrawala, A. (2005). The Horus WLAN Location Determination System. In *Proceedings of the 3rd International Conference on Mobile Systems, Applications, and Services*, MobiSys '05, pages 205–218, New York, NY, USA. ACM. pages 35

Yu-liang, Z. (2013). Multimode-fingerprint matching based indoor positioning system design and implementation. *Computer Engineering and Design*. pages 36

Zhou, C., Yuan, J., Liu, H., and Qiu, J. (2017). Bluetooth indoor positioning based on rssi and kalman filter. *Wireless Personal Communications*, 96:1–16. pages 10

Zhuang, Y., Yang, J., Li, Y., Qi, L., and El-Sheimy, N. (2016). Smartphone-based indoor localization with bluetooth low energy beacons. *Sensors*, 16:596. pages 5

Zuo, J., Liu, S., Xia, H., and Qiao, Y. (2018). Multi-phase fingerprint map based on interpolation for indoor localization using ibeacons. *IEEE Sensors Journal*, 18(8):3351–3359. pages 2